Available online at www.sciencedirect.com
ScienceDirect
Thin Solid Films 516 (2008) 5052–5056
www.elsevier.com/locate/tsf

Transparent conducting F-doped SnO_2 thin films grown by pulsed laser deposition

H. Kim*, R.C.Y. Auyeung, A. Piqué

Naval Research Laboratory, 4555 Overlook Ave, SW, Washington DC 20375, USA

Received 24 July 2007; received in revised form 7 November 2007; accepted 15 November 2007
Available online 23 November 2007

Abstract

Transparent conducting fluorine-doped tin oxide (SnO_2:F) films have been deposited on glass substrates by pulsed laser deposition. The structural, electrical and optical properties of the SnO_2:F films have been investigated as a function of F-doping level and substrate deposition temperature. The optimum target composition for high conductivity was found to be 10 wt.% SnF_2+90 wt.% SnO_2. Under optimized deposition conditions (T_s=300 °C, and 7.33 Pa of O_2), electrical resistivity of 5×10^{-4} Ω-cm, sheet resistance of 12.5 Ω/□, average optical transmittance of 87% in the visible range, and optical band-gap of 4.25 eV were obtained for 400 nm thick SnO_2:F films. Atomic force microscopy measurements for these SnO_2:F films indicated that their root-mean-square surface roughness (~6 Å) was superior to that of commercially available chemical vapor deposited SnO_2:F films (~85 Å).
Published by Elsevier B.V.

PACS: 61.80.B; 68.47.Fg; 72.20.-i; 78.20.-e
Keywords: Fluorine-doped tin oxide; Pulsed laser deposition; Transparent electrode; Surface morphology

1. Introduction

Doped tin oxide (SnO_2) films have been widely used as transparent conducting electrodes in many optoelectronic and electro-optic devices such as solar cells [1,2] and flat panel displays [3,4] due to their high electrical conductivity and high optical transmittance in the visible, and high infrared reflectance. Compared to the more widely used indium tin oxide (ITO), SnO_2 films are inexpensive, chemically stable in acidic and basic solutions, thermally stable in oxidizing environments at high temperatures, and also mechanically strong, which are important attributes for the fabrication and operation of solar cells. Many dopants, such as antimony (Sb), arsenic (As), phosphorus (P), indium (In), molybdenum (Mo), fluorine (F), and chlorine (Cl), have been studied to improve the electrical and optical properties of SnO_2 films [5–11]. Among these, Sb and F are found to be the most commonly used dopants for photovoltaic devices in terms of a manufacturing point of view. Highly conductive SnO_2 films can be achieved by substitution of either Sb^{5+} ions at Sn^{4+} cation sites or F^- ions at O^{2-} anion sites in the lattice creating extra electron carriers. Compared to Sb-doping, F-doping is preferred because its excess amount is volatile, while Sb at high doping levels tends to form segregated clusters in the lattice, causing a darkening of the films. For this reason, higher mobility values can normally be observed for F-doped SnO_2 films compared to Sb-doped SnO_2 films, resulting in much lower resistivity SnO_2 films without compromising their optical transmittance [11].

There are numerous deposition techniques used to grow SnO_2 films (either doped or undoped) including chemical vapor deposition (CVD) [12,13], spray pyrolysis [14,15], thermal evaporation [16], sol–gel [17] and sputtering [8,18,19]. However, in order to obtain low resistivity films, these techniques require either high temperature in-situ deposition processes (400–600 °C) or a post-deposition annealing treatment of the deposited films also at high temperatures (400–700 °C). These high temperature treatments limit their use as a top contact layer in amorphous Si-based solar cells and other types of thin-film solar cells. Other techniques, such as pulsed laser deposition (PLD) might be used to achieve high quality SnO_2 films, however, the growth of F-doped SnO_2 films

* Corresponding author. Also at Nova Research Inc.
E-mail address: Heungsoo.kim@nrl.navy.mil (H. Kim).

0040-6090/$ - see front matter. Published by Elsevier B.V.
doi:10.1016/j.tsf.2007.11.079

by PLD has not yet been reported. PLD films crystallize at relatively lower substrate temperatures compared to other physical vapor deposition (PVD) processes due to the high kinetic energies (>1 eV) of the ejected species in the laser-produced plasma [20–22]. In this paper, we report a study of the structural, electrical and optical properties of SnO_2:F thin films deposited by PLD on glass substrates as a function of F-doping level and substrate deposition temperature.

2. Experimental details

SnO_2:F thin films were deposited on glass substrates (2.5 cm × 2.5 cm × 0.1 cm: Corning 1737) using a KrF excimer laser (Lambda Physik LPX 305, 248 nm, 30 ns full width at half maximum). The laser was operated at 10 Hz and was focused through a 50-cm focal length lens onto a rotating target at a 45° angle of incidence. The energy density of the laser beam at the target surface was maintained at 1.5 J/cm^2. The target-to-substrate distance was 5.8 cm. The targets were prepared from SnO_2 (purity, 99.99%) and SnF_2 (purity, 99.9%) powders [Alfa *AESAR*]. The powders were mixed in a mechanical shaker for 1 h, pressed into a 2.5 cm diameter pellet at 10,000 kg at 120 °C, and then sintered at 200 °C for 48 h in air. The substrates were carefully cleaned in an ultrasonic bath for 10 min with acetone and then methanol. Films were deposited at substrate temperatures ranging from 25 °C to 500 °C in oxygen partial pressure of 7.33 Pa (~55 mTorr).

The film thickness was measured by a stylus profilometer [P-10 KLA Tencor]. A thickness variation of ~10% was observed over a 2 × 2 cm^2 substrate area. This variation was determined after several measurements accross randomly selected locations. The sheet resistance (R_s) was determined by four-point probe measurements. By assuming that the thickness of the films was uniform (<5% variation), the film resistivity (ρ) was calculated using the simple relationship: $\rho = R_s \cdot t$, where t is the film thickness. Hall-effect measurements were carried out using a Quantum Design physical property measurement system. The Hall voltage (V_h) was examined with magnetic fields from −10 to +10 kG, and the results were corrected to compensate for magnetoresistance effects. The Hall coefficient (R_h) was calculated from the relationship: $R_h = (V_h \cdot A)/(I \cdot l \cdot B)$, where A is the cross sectional area through which the current passes, l is the voltage lead separation, and B is the applied magnetic field. The optical transmittance measurements were performed using a UV–visible-near IR spectrophotometer [Perkin-Elmer Lambda 9]. All transmittance values were normalized by the values of the bare glass substrate. X-ray diffraction (XRD) [Rigaku rotating anode X-ray generator with CuK_α radiation] was used to characterize the crystal structure of the films. Atomic force microscopy (AFM) [Digital Instrument, Dimension 3100 series] was used to evaluate the surface morphology of the films.

3. Results and discussion

Fig. 1a shows the X-ray diffraction patterns for undoped SnO_2 and SnO_2:F films grown on glass substrates at 300 °C in 7.33 Pa of oxygen. It can be seen that all the films are polycrystalline and contain the SnO_2 tetragonal structure [23]. All the films exhibit the preferred orientation with a (200) plane while all targets are polycrystalline with the highest intensity reflection corresponding to the (110) peak. Similar (200) preferred orientation has been observed by other groups [14,15] with SnO_2:F films grown by spray pyrolysis. It is also noted that a high intensity peak corresponding to the (211) plane is observed for the undoped SnO_2 film and a relatively low intensity peak from the (211) plane is observed for the F-doped SnO_2 films. The grain size of the deposited films was calculated by the Scherrer formula [24] from the XRD peaks to be 24–30 nm. The lattice parameters (a and c) calculated from the XRD patterns for undoped SnO_2 and doped SnO_2:F films are shown in Table 1. For all films, the 'a' lattice parameter values are larger than that of the SnO_2 powder (a=4.738 Å), while for the doped films (5–20%) the 'c' values are larger than that of the SnO_2 powder (c=3.187 Å). Although the volume of the unit

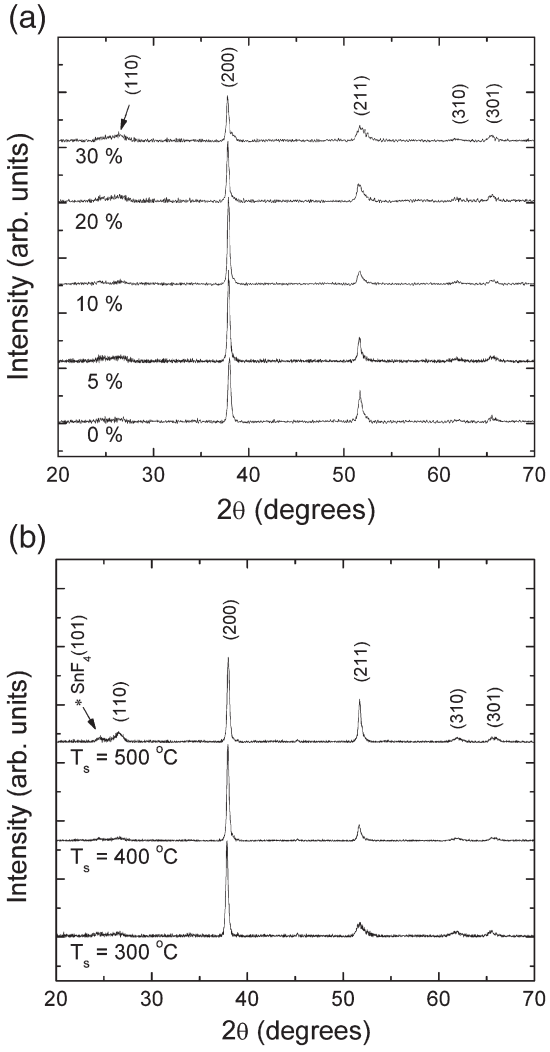

Fig. 1. (a) X-ray diffraction (XRD) patterns as a function of SnF_2 content in the target for undoped SnO_2 (0%) and F-doped SnO_2 (5–30%) films. All films were grown by PLD on glass substrates at 300 °C in 7.33 Pa of oxygen. (b) XRD patterns as a function of substrate deposition temperature for SnO_2:F films grown at 7.33 Pa of O_2. The film thickness is ~450 nm for all films.

Table 1
Lattice parameter and volume data of the unit cells for undoped and F-doped SnO_2 films

SnF_2 (wt.%)	a (Å)	c (Å)	V(Å^3)
SnO_2 powder [23]	4.7382	3.1871	71.55
0	4.7590	3.1819	72.06
5	4.7605	3.2023	72.57
10	4.7543	3.2179	72.74
20	4.7724	3.1918	72.72
30	4.8113	3.1090	71.98

cell for all the films grown by PLD in this work is observed to be larger than that of the SnO_2 powder, it is clear that the volume of the unit cell is not significantly affected by F doping. Since the ionic radius of F^- (1.33 Å) is slightly larger than that of O^{2-} (1.32 Å), the small change in the lattice volume is probably due to the incorporation of F ions into the O ion sites. This change of lattice parameters is also related to oxygen deficiency [19] and strain effects due to the thermal expansion coefficient mismatch between the film (5×10^{-6}/ °C) [25] and glass substrate (4.6×10^{-6}/°C).

As seen in Fig. 1(b), the substrate deposition temperature (T_s) also affects the preferred orientation of SnO_2:F films. At T_s=300 °C, the SnO_2:F film shows the (200) preferred orientation with a low intensity peak from the (211) plane. However, when T_s increases, the intensity of the (211) peak increases. The intensity ratio of (211) to (200) varies from 0.21 to 0.78 with an increase in the T_s from 300 °C to 500 °C. The temperature dependence of the preferred orientation was also reported by other research groups for SnO_2:F films grown by spray pyrolysis [14]. The calculated grain size increases from 28 nm to 41 nm with an increase in the T_s from 300 °C to 500 °C.

Doping of SnO_2 films with fluorine improves their electrical properties. Fig. 2 shows the variation of electrical resistivity (ρ), carrier concentration (n), and Hall mobility (μ) of SnO_2:F films as a function of a SnF_2 content in the target. The films were deposited at 300 °C and 7.33 Pa of oxygen. It is observed that the resistivity initially decreases with the SnF_2 content, reaches a minimum at the 10 wt.% of SnF_2 ($\rho\sim5\times10^{-4}$ Ω-cm), and slightly increases as the SnF_2 content in the target is augmented beyond 10 wt.%. The initial decrease in resistivity is attributed to an increase in free carrier concentration due to the substitutional incorporation of F^- ions at O^{2-} anion sites. However, for films with higher SnF_2 content (10–50%), the free carrier concentration saturates and the mobility slightly decreases due to the formation of Sn–F complexes in the grain boundaries, leading to a slight increase in the resistivity of the SnO_2:F films.

The dependence of the electrical resistivity (ρ), carrier concentration (n), and Hall mobility (μ) of SnO_2:F films on the substrate deposition temperature (T_s) is shown in Fig. 3. All SnO_2:F films in Fig. 3 were deposited from a 10 wt.% of SnF_2-doped SnO_2 target at 7.33 Pa of oxygen. The resistivity initially decreases with T_s, reaches a minimum at 300 °C, and increases with further increasing T_s up to 500 °C. The initial decrease in resistivity is due to an increase of both free carrier concentration and Hall mobility. The initial increase of carrier concentration with T_s is related to an increase in diffusion of F^- ions into the O^{2-} anion sites. The initial increase in Hall mobility can be explained by the fact that the grain size increases with increasing T_s, thus reducing the grain boundary scattering and decreasing the resistivity. At higher temperatures (300–500 °C), the resistivity is observed to increase because of loss of F^- ions in the film or contamination of the film by alkaline ions from the glass substrate [26]. Compared to the SnO_2:F films grown by other techniques (optimum T_s=400–450 °C) [14,27], the optimum deposition temperature for PLD grown films is rather low (~300 °C). For example, Shanthi et al. [27] have grown SnO_2:F films by spray pyrolysis and found that the resistivity decreases with the T_s up to ~400 °C and increases thereafter. The carrier concentration and carrier mobility show a maximum at the same temperature (400 °C). This influence of the substrate

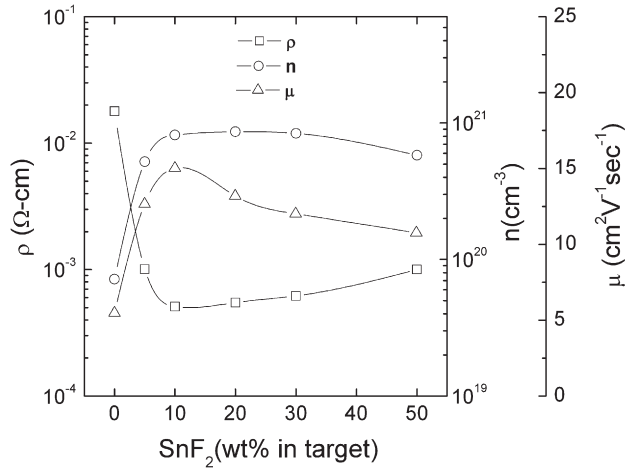

Fig. 2. Variation of electrical resistivity (ρ), carrier concentration (n), and Hall mobility (μ) as a function of SnF_2 content in the target for SnO_2:F films deposited on glass substrates at 300 °C in 7.33 Pa of oxygen. The film thickness is ~450 nm for all films.

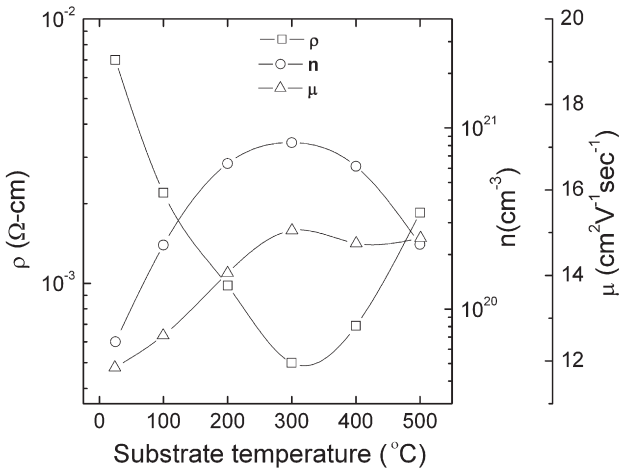

Fig. 3. Variation of electrical resistivity (ρ), carrier concentration (n), and Hall mobility (μ) of SnO_2:F films as a function of substrate deposition temperature. All films were deposited on glass substrates from a 10 wt.% SnF_2-doped SnO_2 target at 7.33 Pa of oxygen. The film thickness is ~450 nm for all films.

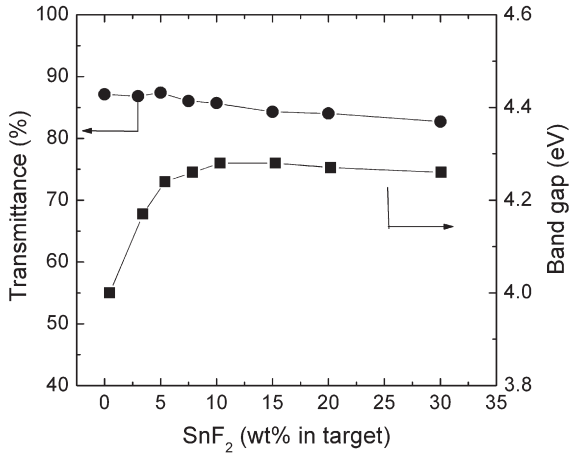

Fig. 4. Optical transmittance and direct band-gap of SnO_2:F films as a function of SnF_2 content in the target. All films were grown by PLD on glass substrates at 300 °C in 7.33 Pa of oxygen. The optical transmittance values are obtained as an average value in the visible range (400–800 nm).

deposition temperature is similar to our present results except for the higher optimum temperature.

The optical transmittance (T) data were used to calculate the absorption coefficient (α) of the films using the relation: $T \approx \exp(-\alpha t)$, where t is the film thickness. The absorption coefficient data was used to determine the optical band-gap (E_g) using the relation: $\alpha h\nu \approx (h\nu - E_g)^{1/2}$,where $h\nu$ is the photon energy. The direct optical band-gap was determined by extrapolating the straight regions of the plots of α^2 vs. $h\nu$ to $\alpha^2 = 0$ (i.e., $\alpha h\nu = 0$) [28]. Fig. 4 shows the variation of average transmittance in the visible range (400–800 nm) and direct band-gap as a function of a SnF_2 content in the target for SnO_2:F films deposited at 300 °C and 7.33 Pa for oxygen. The transmittance values are observed to slightly decrease with increasing F concentration in the target. This is attributed to an increase of the carrier concentration in the films as a result of F doping. The E_g values are found to initially increase with increasing the SnF_2 content up to 10 wt.% and then become independent of SnF_2 content up to 30 wt.%. This shift of band-gap with the F-doping amount (i.e., the carrier concentration) can be explained by the Burstein–Moss (B–M) shift; the absorption edge shifts towards higher energy with an increase of carrier concentration [29,30]. However, above the critical F-doping level (~10 wt.% of SnF_2), the E_g values decrease slightly due to a small decrease in carrier concentration. Similar B–M shifts have been reported by other research groups for the SnO_2:F films grown by spray pyrolysis [14].

The substrate deposition temperature (T_s) also affects the optical properties of the SnO_2:F films. Fig. 5 shows the variation of average transmittance in the visible range (400–800 nm) and direct band-gap as a function of the T_s for SnO_2:F films deposited from a 10 wt.% of SnF_2-doped SnO_2 target at 7.33 Pa of oxygen. The optical transmittance in the visible range increases noticeably from 65% to 87% as the T_s raises from 25 °C to 300 °C and slightly increases to 90% with a further raise in T_s up to 500 °C. It is observed that the direct band-gap increases from 3.65 eV to 4.25 eV with an increase in the deposition temperature from 25 °C to 300 °C. This increase in band-gap can be attributed to an increase in carrier concentration of the films. With a further increase of the T_s to 500 °C, the optical band-gap slightly decreases to 4.21 eV. Similar optical band-gap values were previously reported (3.5–4.41 eV) for the

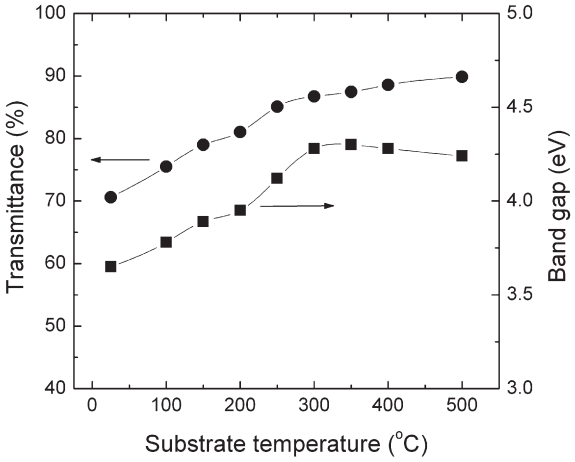

Fig. 5. Optical transmittance and direct band-gap of SnO_2:F films as a function of substrate deposition temperature. The optical transmittance values are obtained as an average value in the visible range (400–800 nm). All films were deposited on glass substrates from a 10 wt.% SnF_2-doped SnO_2 target at 7.33 Pa of oxygen.

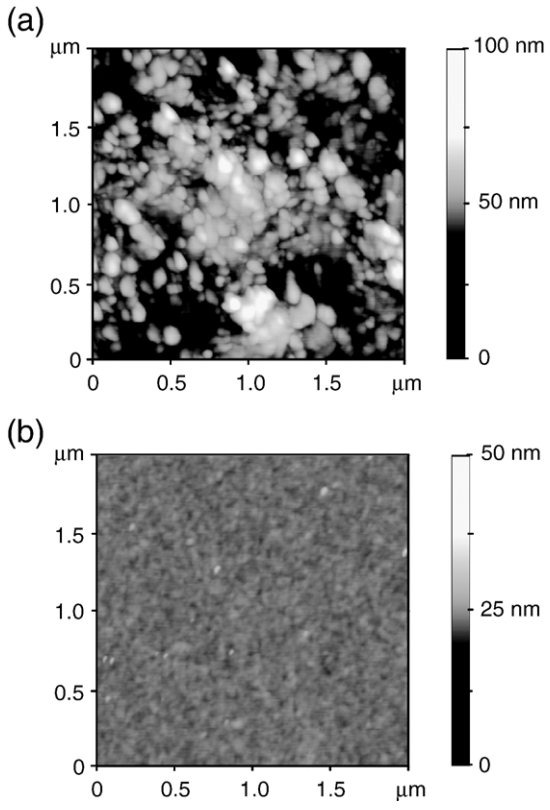

Fig. 6. AFM images (2 μm × 2 μm) of SnO_2:F films grown on glass substrates by (a) CVD (supplied by Pilkington TEC Glass) and (b) PLD (this work). The AFM measurements were performed near the center region of the films. The film thickness is ~400 nm for both samples. The PLD film was grown at 300 °C in 7.33 Pa of oxygen.

SnO_2:F films [14,27]. The refractive index values of all SnO_2:F films used in this investigation are in the range from 1.91 to 2.04 at the wavelength of 550 nm.

The surface morphology of the transparent electrodes is another important factor in order to achieve high device performance in many applications such as photovoltaics and flat panel displays where the SnO_2:F layer is to be used as an electrode. Fig. 6 shows 2-D AFM images of SnO_2:F films deposited by CVD (supplied by Pilkington TEC Glass) and PLD (this work). The sheet resistance values of the films grown by CVD and PLD are ~14 Ω/□ and ~12.5 Ω/□, respectively. Prior to the AFM measurements, the films were ultrasonically cleaned in methanol and blown dry with nitrogen gas. It is clear that the films grown by PLD are much smoother than the commercial films grown by CVD. The root-mean-square (rms) surface roughness of a typical PLD film is ~6 Å, while the rms surface roughness of the commercial CVD film is ~85 Å. The PLD grown SnO_2:F films with a surface morphology over an order of magnitude smoother than currently available commercial SnO_2:F films should allow for developing higher efficiency devices such as organic light-emitting diodes and organic photovoltaic cells. Furthermore, since the PLD films crystallize at relatively low temperatures, the PLD grown SnO_2:F films can be used to make high quality transparent electrodes on plastic substrates for flexible device applications. Investigation of the growth of SnO_2:F films on plastic substrates is currently being pursued by our group.

4. Conclusion

High quality SnO_2:F films were grown on glass substrates by pulsed laser deposition. The structural, electrical and optical properties of the SnO_2:F films were investigated as a function of doping level and substrate deposition temperature. For a 400 nm thick SnO_2:F film deposited at T_s=300 °C and 7.33 Pa of oxygen, an electrical resistivity of 5×10^{-4} Ω-cm with an average optical transmittance of 87% in the visible range was measured. AFM measurements indicated that the rms surface roughness of the PLD grown SnO_2:F films (~6 Å) was over an order of magnitude smoother than that of commercially available CVD SnO_2:F films (~85 Å). This work has shown the ability to grow SnO_2:F films with low resistivity, high optical transmission and low rms surface roughness at low deposition temperatures (≤300 °C) by PLD. This is of great importance for the fabrication of high quality transparent electrodes on plastic substrates for flexible devices and as top contact layers for high efficiency photovoltaics like those in thin-film solar cells.

Acknowledgements

This work was supported by Office of Naval Research (ONR).

References

[1] B. O'Regan, M. Grätzel, Nature 353 (1991) 737.
[2] H. Kim, G.P. Kushto, C.B. Arnold, Z.H. Kafafi, A. Pique, Appl. Phys. Lett. 85 (2004) 464.
[3] T. Fukano, T. Motohiro, T. Ida, H. Hashizume, J. Appl. Phys. 97 (2005) 084314.
[4] W. Brütting, M. Meier, M. Herold, S. Krag, M. Schwoerer, Chem. Phys. 227 (1998) 243.
[5] H. Kim, A. Piqué, Appl. Phys. Lett. 84 (2004) 218.
[6] S.R. Vishwakarma, J.P. Upadhyay, H.C. Prasad, Thin Solid Films 176 (1989) 99.
[7] J.P. Upadhyay, S.R. Vishwakarma, H.C. Prasad, Thin Solid Films 167 (1988) 7.
[8] B. Stjerna, E. Olsson, C.G. Granqvist, J. Appl. Phys. 76 (1994) 3797.
[9] P.K. Manoj, B. Joseph, V.K. Vaidyan, D.S.D. Amma, Ceramic International 33 (2007) 273.
[10] S. Suporthina, M.R. De Guire, Thin Solid Films 371 (2000) 1.
[11] H.L. Hartnagel, A.L. Dawar, A.K. Jain, C. Jagadish, Semiconducting Transparent Thin Films, Institute of Physics Publishing, Bristol, 1995.
[12] C. Arias, L.S. Roman, T. Bugler, R. Tomfool, M.S. Moravia, I.A. Hummel, Thin Solid Films 371 (2000) 29.
[13] A. Rakhshani, Y. Makdish, H. Ramazaniyan, J. Appl. Phys. 83 (1998) 1049.
[14] A. Martinez, D.R. Acosta, Thin Solid Films 483 (2005) 107.
[15] B. Thangaraju, Thin Solid Films, 402 (2002) 71.
[16] D. Das, R. Banerjee, Thin Solid Films 147 (1987) 321.
[17] O.K. Varghese, L.K. Malhotra, J. Appl. Phys. 87 (2000) 7457.
[18] Y. Onuma, Z. Wang, H. Ito, M. Nakao, K. Kamimura, Jpn. J. Appl. Phys. 37 (1998) 963.
[19] B.P. Howson, H. Barakova, A.G. Spencer, Thin Solid Films 196 (1991) 315.
[20] D.B. Chrisey, G.K. Hubler, Pulsed Laser Deposition of Thin Films, Wiley, New York, 1994.
[21] H. Kim, C.M. Gilmore, A. Piqué, J.S. Horwitz, H. Mattoussi, H. Murata, Z.H. Kafafi, D.B. Chrisey, J. Appl. Phys. 86 (1999) 6451.
[22] H. Kim, J.S. Horwitz, G. Kushto, Z.H. Kafafi, D.B. Chrisey, Appl. Phys. Lett. 79 (2001) 284.
[23] Joint Committee on Powder Diffraction Standards, International Centre for Diffraction Data, # 41-1445.
[24] B.D. Cullity, Elements of X-ray Diffraction, 2nd ed. Addison-Wesley, Reading, MA, 1978.
[25] W.F. Wu, B.S. Chiou, Thin Solid Films 293 (1997) 244.
[26] H. Kaneko, K. Miyake, J. Appl. Phys. 53 (1982) 3629.
[27] E. Shanthi, A. Banerjee, V. Dutta, K.L. Chopra, J. Appl. Phys. 53 (1982) 1615.
[28] J. Tauc, R. Grigorovici, A. Vancu, Phys. Status Solidi 15 (1966) 627.
[29] E. Burstein, Phys. Rev. 93 (1954) 632.
[30] T.S. Moss, Proc. Phys. Soc. London, Sect. B 67 (1954) 775.